Photo-activated CO-release in the amino tungsten Fischer carbene complex, [(CO)5WC(NC4H8)Me], picosecond time resolved infrared spectroscopy, time-dependent density functional theory, and an antimicrobial study

McMahon, S.; Rajagopal, A.; Amirjalayer, S.; Halpin, Y.; Fitzgerald-Hughes, D.; Buma, W.J.; Woutersen, S.; Long, C.; Pryce, M.T.

DOI
10.1016/j.jinorgbio.2020.111071

Publication date
2020

Document Version
Final published version

Published in
Journal of inorganic biochemistry

Journal of Inorganic Biochemistry 208 (2020) 111071

Contents lists available at ScienceDirect

Journal of Inorganic Biochemistry

journal homepage: www.elsevier.com/locate/jinorgbio

Photo-activated CO-release in the amino tungsten Fischer carbene complex, $[(CO)_5WC(NC_4H_8)Me]$, picosecond time resolved infrared spectroscopy, time-dependent density functional theory, and an antimicrobial study

Suzanne McMahon[a], Ashwene Rajagopal[a,b], Saeed Amirjalayer[c], Yvonne Halpin[a], Deirdre Fitzgerald-Hughes[b], Wybren Jan Buma[d], Sander Woutersen[d], Conor Long[a], Mary T. Pryce[a,*]

[a] School of Chemical Sciences, Dublin City University, Dublin 9, Ireland
[b] Clinical Microbiology, Royal College of Surgeons in Ireland, RCSI Education and Research, Beaumont Hospital, Beaumont, Dublin 9, Ireland
[c] Physikalisches Institut, Center for Nanotechnology (CeNTech) and Center for Multiscale Theory & Computation (CMTC), Westfälische Wilhelms-Universität Münster, Heisenbergstrasse 11, 48149 Münster, Germany
[d] University of Amsterdam, Van't Hoff Institute for Molecular Sciences, Science Park 904, 1098 XH, Amsterdam, P.O. Box 94157, 1090 GD Amsterdam, The Netherlands

ARTICLE INFO

Keywords:
Tungsten based Fischer carbene
Photochemical CO-loss
Antimicrobial
Picosecond time-resolved infrared spectroscopy

ABSTRACT

Picosecond time-resolved infrared spectroscopy was used to probe the photo-induced early state dynamics preceding CO loss in the Fischer carbene complex, $[(CO)_5WC(NC_4H_8)CH_3]$. Time-dependent density functional theory calculations were employed to help in understanding the photochemical and photophysical processes leading to CO-loss. Electrochemical initiated CO release was quantified using gas chromatography. The potential of $[(CO)_5WC(NC_4H_8)CH_3]$, as an antimicrobial agent under irradiation conditions was studied using a *Staphylococcus aureus* strain.

1. Introduction

Fischer carbene complexes have been used widely as reagents in various organic transformations, and in organometallic synthesis, using both thermal and photochemical approaches [1–5]. Fischer carbene complexes of group 6 metals have been shown to react under photochemical conditions with imines, alkenes, aldehydes or alcohols producing a wide variety of useful compounds including β-lactams, β-lactones, cyclobutanones, or amino esters [6–9]. Recently low temperature matrix isolation and time resolved spectroscopy has been used in identifying the various intermediates generated in these processes. In 1988, Hegedus and co-workers, proposed that visible light irradiation results in photocarbonylation of alkoxy Fischer carbenes, via either a short lived metallocyclopropanone or a metallaketene intermediate [10–12]. We and others have used picosecond time-resolved infrared spectroscopy to confirm the formation of a metallaketene intermediate species [13,14]. Fischer carbene complexes containing alkoxy groups on the carbene carbon, such as $[(CO)_5MC(OMe)Me]$ (M = Cr or W), undergo *anti-syn* isomerisation of the alkoxy substituent following low energy photolysis. Increasing the excitation energy, however, can result in the formation of a reactive metallaketene intermediate (100 ps) in the case of the chromium analogue. This excited state was detected using picosecond time-resolved infrared spectroscopy (psTRIR) [13], and supported by quantum chemical calculations. For M = Cr, time-dependent density functional theory (TDDFT) calculations indicate that the metallaketene-chromium intermediate has singlet character, while in the case of the tungsten analogue, the metallaketene intermediate is produced from a triplet state [13,15]. In addition, to these two process, the alkoxy based Fischer carbene compounds also undergo photo-induced CO-loss following higher energy photolysis [16,17]. Previously we have shown that replacement of the alkoxy group by an amino substituent (pyrrolidine), greatly enhances the quantum efficiency for CO loss, and the photon energy required to achieve CO-loss is greatly reduced [18]. For example, when $[(CO)_5CrC(NC_4H_8)(Me)]$ was irradiated at λ = 400 nm, rapid (< 50 ps) CO loss occurs, with a quantum yield of approximately 70%. No evidence was obtained for the formation of metallaketene intermediates or metallacyclopropanone excited states with this system, which is not surprising as amino Fischer carbene complexes are known to be poor reagents in the synthesis of β-lactams. Among the very few reports on the photochemistry of tungsten based amino Fischer carbene complexes Rooney et al. used Raman spectroscopy, to identify $[(CH_3CN)(CO)_4WC(NC_4H_8)(SiPh_3)]$ following

* Corresponding author at: School of Chemical Sciences, Dublin City University, Ireland.
E-mail address: mary.pryce@dcu.ie (M.T. Pryce).

https://doi.org/10.1016/j.jinorgbio.2020.111071
Received 1 December 2019; Received in revised form 19 March 2020; Accepted 19 March 2020
Available online 07 May 2020

excitation of [$(CO)_5WC(NC_4H_8)(SiPh_3)$] in acetonitrile [19]. While the synthetic applications of Fischer carbenes are well known, more recently metal carbonyls have been studied for both antimicrobial effects and therapeutic applications [20]. The toxic effects of inhaled environmental CO are well known, but surprisingly the important role of CO as an intracellular messenger, regulating physiological and cryoprotective processes in the body is less understood [21]. The positive effects of CO, which may have clinical applications include vasodilation, anti-inflammatory, anti-proliferative and anti-apoptotic activities [22]. However, for clinical applications, controlling the delivery of CO gas is essential but challenging. Harnessing CO, in CO-releasing compounds (CO-RMs) where a light or electrochemical stimuli can be used to break bonds and liberate "free CO" has been suggested as a means to control delivery for clinical applications [23,24]. Light induced CO release from molecules (photo-CORMS) may facilitate controlled timing, dosage and location of CO release for on-target applications [25,26]. The development of photoCORMs includes compounds absorbing in the ultraviolet, the visible region, and ideally into the therapeutic window [27]. The photochemistry of a wide range of metal carbonyls have been studied in aqueous media, from the original studies which focused on $Fe(CO)_5$ and $Mn_2(CO)_{10}$ [28], to others containing for example tripodal, di-imine or bipyridine type ligands, and including metal centers such as Mo, W, Re or Ru [29–42]. The antimicrobial properties of metal carbonyl compounds against both *E. coli* and *S. aureus* were reported by Nobre and co-workers who demonstrated the superior bactericidal activity of CORMs versus using solely carbon monoxide gas [43]. Following these initial antimicrobial studies, many other metal carbonyls compounds based on Mn, Fe and Cu have been assessed for bactericidal properties, both in the presence and absence of a light source [44–47,50–54]. Chromium based Fischer carbene complexes have previously been studied as CO-releasing modalities in the absence of light in aqueous media where myoglobin was used to quantify CO. [34] Under the conditions employed, nucleophilic attack by water was reported to be important for CO loss, and a clear correlation between the electrophilicity of the carbene carbon and the rate of CO release in solution was reported. In this study, we report the results from a ps-TRIR investigation on the [$(CO)_5WC(NC_4H_8)CH_3$] compound combined with an electrochemical study where induced CO loss is confirmed using gas chromatography. Similarly, to the chromium analogue, the tungsten amino Fischer carbene complex, undergoes efficient CO-loss using 400 nm excitation, with no evidence for the formation a metallaketene intermediate from the time resolved studies [13,18]. The photochemistry and the high quantum yield for CO-loss is supported using TDDFT calculations. Furthermore, the potential application of the compound as an antimicrobial agent was assessed using a *Staphylococcus aureus* strain (ATCC 25923).

2. Materials and instrumentation

2.1. UV–vis spectroscopy

UV–vis spectra were measured on an Agilent 8453 UV–vis spectrophotometer in a 1 cm quartz cell using spectroscopic grade solvents.

2.2. NMR spectroscopy

^1H NMR was recorded on a Bruker AC 400 spectrophotometer in $CDCl_3$ and were calibrated according to the deuterated solvent peak.

2.3. Picosecond time-resolved infrared spectroscopy

The TRIR experiments were performed at the University of Amsterdam. UV pump and mid-IR probe pulses were generated by a Ti:sapphire laser with a repetition rate of 1 kHz were utilised. The UV pump pulse (400 nm) was generated by second harmonic generation (SHG). Typical pulse energies employed were 0.8–1.0 μJ. IR probe pulses were generated by difference frequency generation (DFG) of the signal and idler from a β-barium borate (BBO)-based optical parametric amplifier (OPA) in $AgGaS_2$. The delay between pump and probe was scanned by mechanically adjusting the beam-path of the UV pump using a translation stage. The temporal resolution of 200 fs has been obtained from the full width at half maximum (FWHM) of the pump-probe cross-correlate function. Solutions were continually circulated (flowed) through IR cells containing CaF_2 windows with a path length of 500 μm.

2.4. Cyclic voltammetry and electrochemical loss

Cyclic voltammetry (CVs) and bulk electrolysis profiles were recorded in anhydrous acetonitrile (Sigma-Aldrich) with tetrabutylammonium hexafluorophosphate ($TBAPF_6$) (0.1 M), as a supporting electrolyte. The concentration of the sample was 0.001 M throughout. Experiments were carried out using a CH Instruments 750C electrochemical potentiostat. All electrochemical experiments were performed at room temperature (20 °C) unless stated otherwise. A three-electrode cell was employed which consisted of a glassy carbon working electrode, a Pt wire auxiliary electrode and Ag/AgCl reference electrode ($E_{1/2}$ Fc/Fc^+ redox couple = + 0.43 V). The scan rate was 0.1 Vs^{-1} unless otherwise stated. All experiments were performed with the cell in the absence of light. CO release was detected using a Shimadzu GC-2010 Plus unit (Lab Solutions version 5.57 software) with a dielectric barrier discharge ionisation detector (BID) and a ShinCarbon micropacked column with 0.53 mm internal diameter.

2.5. Computational studies

All calculations were performed using the Gaussian 16 (Revision B.01) program suite [55], using the exchange functional of Becke [56] and the correlation functional of Lee Yang and Parr [57,58] i.e. the B3LYP method and a triple zeta quality basis set def2-TZVP [59,60]. All molecular geometries were optimised to tight convergence criteria, and different solvent environments were modelled using a polarisable continuum model [61]. Relaxed potential energy scans were undertaken along the chosen reaction coordinates, providing sets of atomic coordinates at each point, which were then used to calculate the excited state energies of both singlet and triplet excited states using Time-Dependent Density Functional Theory (TDDFT) [62,63].

2.6. General remarks

All chemicals were purchased from Sigma Aldrich, ABCR or ACROS and were of reagent grade. The chemicals were used without further purification.

2.7. Synthesis

2.7.1. Preparation of $[(CO)_5WC(NC_4H_8)Me]$

The synthesis of [$(CO)_5WC(NC_4H_8)$Me] was carried out according to previously reported procedures [64,65]. 0.31 mmol (0.026 mL) of pyrrolidine was added via syringe to a solution of [$(CO)_5WC(OMe)$Me] [66] (0.26 mmol, 0.100 g) in diethyl ether (15 mL) at −78 °C (this temperature was achieved by combining liquid nitrogen and acetone and monitored using an alcohol thermometer). The reaction was stirred and allowed to reach room temperature. The solution changed from a bright yellow colour to cream. The solvent and any excess pyrrolidine were removed at reduced pressure. The crude complex was purified on a silica gel column using a solvent mix of pentane:dichloromethane (9:1). The spectroscopic data was in agreement with reported data [19,20].

2.8. Antimicrobial evaluation

The antimicrobial activity of $[(CO)_5WC(NC_4H_8)Me]$ was assessed using a *Staphylococcus aureus* reference strain, (ATCC 25923). Bacteria were grown overnight at 37 °C on Mueller-Hinton (MH) agar and suspensions were prepared from isolated colonies to the density of a 0.5 McFarland standard (bioMèrieux, Ireland) and were further diluted 1/100 in phosphate buffered saline (PBS), pH 7.4 (approximately 1×10^6 CFU/ml, where CFU is colony forming units). Assays were prepared in micro centrifuge tubes and contained approximately 1×10^5 CFU/ml of bacteria and varying concentrations of tungsten carbonyl carbene complex (50–200 μM in 10% DMSO) in PBS. Control assays contained no complex and a DMSO control was also included. For irradiation, 100 μl aliquots were transferred to the wells of a 96 well tissue culture plate which was irradiated for 1 h using a LED lamp with wavelength ($\lambda_{exc.} \sim 355$ nm). For non-irradiated controls, aliquots were transferred to another 96-well plate which was incubated in the dark for 1 h. The contents of the wells were then diluted, 1/100 with PBS and 100 μl spread onto MH agar and incubated at 37 °C overnight before counting colony forming units (CFU). For irradiated and non-irradiated assays, the percentage killing activity was calculated based on the CFU/mL from treated bacteria compared to untreated (control assays containing DMSO). To confirm the contribution of CO to bactericidal activity, assays were performed in the presence of a CO scavenger, bovine haemoglobin at 20 μM for comparison (see ESI).

3. Results and discussion

The UV–vis spectrum of $[(CO)_5WC(NC_4H_8)Me]$ in *n*-heptane is presented in Fig. 1. The main features of this spectrum are an absorption maximum at 337 nm and a shoulder at 364 nm. The spectrum is consistent with those of other Fischer carbene complexes reported in the literature [19,67]. Superimposed on the experimental spectrum are the vertical excitation energies to singlet excited states (represented by black lines) calculated by TDDFT methods and the excitation wavelength used in the TRIR studies (400 nm) is indicated by a downward arrow. The electron density difference maps for the two singlet excited states close to this wavelength are also presented, and these can be

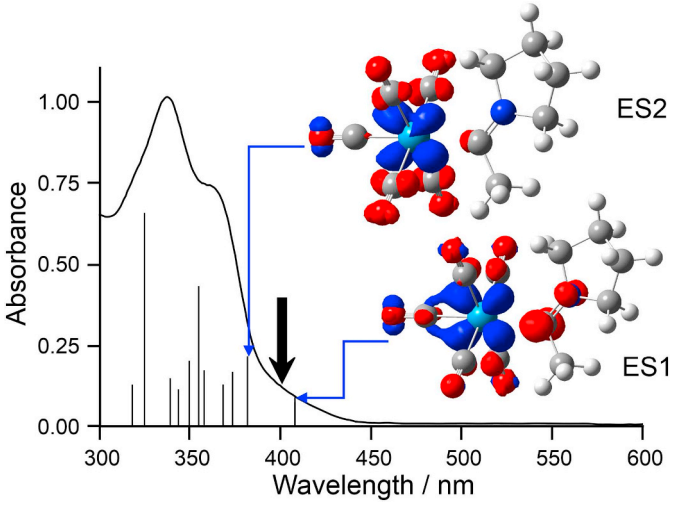

Fig. 1. The UV/vis spectrum of $[(CO)_5WC(NC_4H_8)Me]$ in *n*-heptane solution superimposed on the calculated vertical excitation energies to singlet excited states (vertical black lines, obtained from TDDFT calculations) an d the electron density difference maps for the two lowest energy singlet excited states (^{1}ES1 and ^{1}ES2) with the regions where the electron density is reduced in the excited state compared to the ground state coloured blue, and regions where the electron density is increased in the excited state relative to the ground state coloured red.

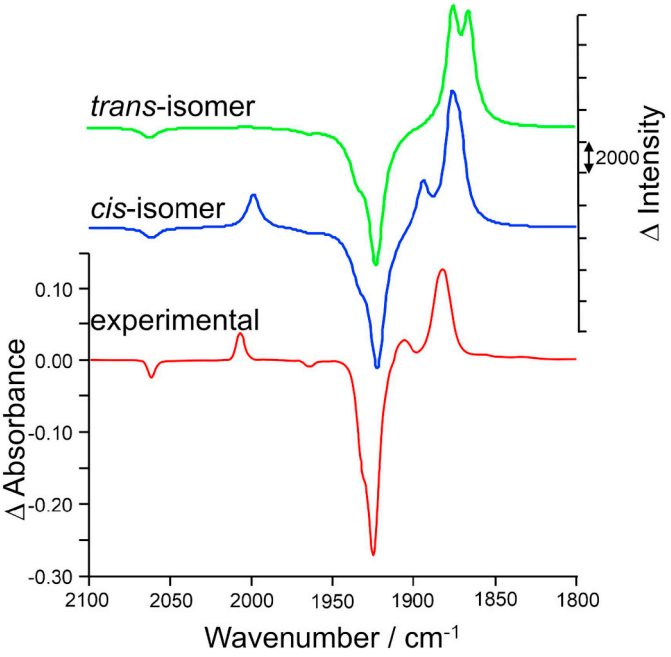

Fig. 2. The red spectrum is the experimental difference spectrum obtained following steady-state (λ_{exc} = 395 nm) photolysis of $[(CO)_5WC(NC_4H_8)Me]$ in *n*-pentane solution in the presence of a trapping ligand (PPh_3, in 1.1 molar equivalent excess). The blue spectrum is the calculated spectrum of *cis*-$[(CO)_4(PPh_3)WC(NC_4H_8)Me]$ minus the spectrum of $[(CO)_5WC(NC_4H_8)Me]$ and the green spectrum represents the calculated spectrum of *trans*-$[(CO)_5WC(NC_4H_8)Me]$ minus the spectrum of $[(CO)_5WC(NC_4H_8)Me]$. All calculated spectra were modelled in *n*-heptane.

characterised as metal-to-carbene (^{1}ES1) and metal-to-*cis*-CO (^{1}ES2) charge-transfer in nature. It is clear from Fig. 1, that irradiation at 400 nm will populate predominantly ^{1}ES1. The behaviour of this excited state was then modelled along either the *cis*- or *trans*-CO loss reaction coordinates (see later).

Prior to performing time resolved studies, steady-state experiments confirmed that photolysis of $[(CO)_5WC(NC_4H_8)Me]$ (λ_{exc} = 395 nm) in *n*-pentane solution, in the presence of the trapping ligand PPh_3, (1.1 molar equivalent excess) produced a CO-loss product $[(CO)_4(PPh_3)WC(NC_4H_8)Me]$ by the appearance of product bands at 2007, 1900, and 1875 cm^{-1}. Two isomeric products are possible from this reaction, either the *cis*- or *trans*-$[(CO)_4(PPh_3)WC(NC_4H_8)Me]$. Modelling of the infrared spectrum of *cis*- or *trans*-products confirmed that the *cis*-isomer is the dominant photoproduct (Fig. 2). It is clear from these results that the band at approximately 2007 cm^{-1} is absent from the spectrum of the *trans*-isomer, and consequently it can be used as a diagnostic feature for the *cis*-CO loss process. These spectral features are consistent with those previously reported for the CO loss photoproduct, $[(pentane)(CO)_4WC(NC_4H_8)SiPh_3]$, which exhibited IR stretching vibrations at 2015, 1923, 1909 and 1856 cm^{-1}, following excitation of $[(CO)_4WC(NC_4H_8)SiPh_3]$ at 355 nm in pentane [19].

3.1. Picosecond time-resolved infrared spectroscopy and time-dependent density functional theory calculations

The photophysical processes leading to CO-loss were studied by calculating the energy profile along two reaction coordinates, *cis*- and *trans*-CO loss, in the ^{1}ES1 state. The ^{1}ES1 state is bound with respect to both of the reaction coordinates (Fig. 3). These TDDFT results show that the barrier for *trans*-CO loss is larger by ~20 kJ mol^{-1} compared to the *cis*-CO loss reaction which explains the dominant formation of the *cis*-CO loss product in the steady-state experiments. Furthermore, the bound nature of this excited state implies that the CO-loss process will

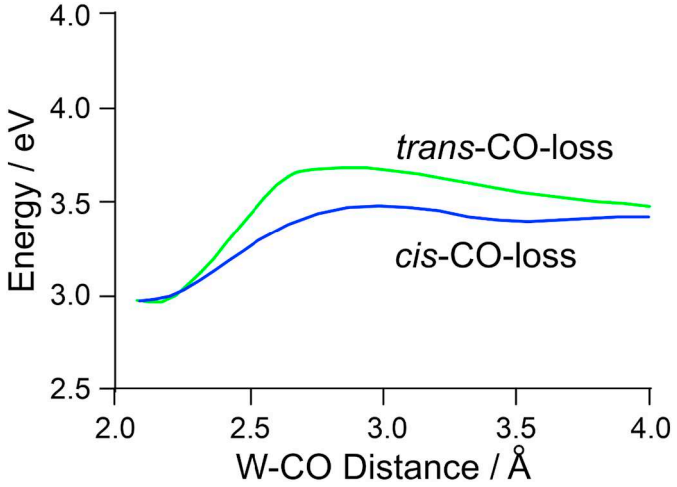

Fig. 3. The non-adiabatic description of the excited state energy change for the ^{1}ES1 as the *cis*-W-CO (blue) and *trans*-W-CO (green) bond length increases showing a lower barrier to *cis*-CO-loss of approximately 20 kJ mol^{-1}.

be "arrested" [68] i.e. it will occur slowly compared to the ultrafast CO-loss following photolysis of, for instance, $Cr(CO)_6$ [69,70].

Based on this, picosecond time-resolved infrared (TRIR) measurements using 400 nm were performed in *n*-heptane solution at room temperature. The ground state FTIR spectrum of $[(CO)_5WC(NC_4H_8)Me]$ exhibits metal carbonyl stretching vibrations at 2063(w), 1967(vw), 1932(s) and 1925(s) cm^{-1}. The very weak parent feature at 1967 cm^{-1} is not evident in the psTRIR experiments. Following excitation at 400 nm, two new intense features at 1906 and 1892 cm^{-1} together with a very weak feature at approximately 2012 cm^{-1} are produced. The IR changes (in the ν_{CO} region) observed in these experiments are consistent with the initial formation of an excited state (^{1}ES1 in Fig. 4). The main IR feature of this excited state was observed at approximately 1892 cm^{-1} (labelled ^{1}ES1 in Fig. 4) which decays over the initial 80 ps, with concomitant formation of bands at 2028, 1911 and 1873 cm^{-1}, which are assigned to the *cis*-$[(CO)_4WC(NC_4H_8)Me]$, i.e. the vacant coordination site on the metal lies *cis* to the carbene ligand. This co-ordinatively unsaturated complex was modelled using DFT methods, and the IR difference spectrum was calculated by subtracting the simulated spectrum of the parent pentacarbonyl complex from the simulated *cis*-CO loss species. This simulated spectrum is also presented as the blue spectrum in Fig. 4. The similarity between this simulated spectrum and the final difference measured at 120 ps after excitation strongly supports characterisation of the main photoproduct as the *cis*-$[(CO)_4WC(NC_4H_8)Me]$ complex.

3.2. Evaluation of CO loss by $[(CO)_5WC(NC_4H_8)Me]$ using cyclic voltammetry

Electrolysis was carried out to determine the efficiency of CO loss for $[(CO)_5WC(NC_4H_8)Me]$, using an electrochemical stimulus compared to a photo-stimulus. As shown in Fig. 5, the compound is oxidised at a potential of +0.52 V vs. Fc/Fc$^+$, an irreversible process at slow scan rates up to 1.0 V/s. This process becomes quasi-reversible at higher scan rates (up to 70 V/s) with an anodic to cathodic peak current ratio of approximately 1:0.5 and is assigned to the metal centered $W^{0/I}$ redox couple as previously reported [71,72]. The oxidation peak is metal-centered whereas the reduction peak points to the metal-carbene double bond. Comparing the oxidation potential of $[(CO)_5WC(NC_4H_8)Me]$ with its Cr analogue, reveals an increase of 180 mV. This behaviour has been shown for other Cr and W based complexes which supports that the oxidation peak is metal-centered [71]. The reduction potential at −2.75 V, vs. Fc/Fc$^+$ is irreversible at the range of scan rates investigated (0.1–50 V/s).

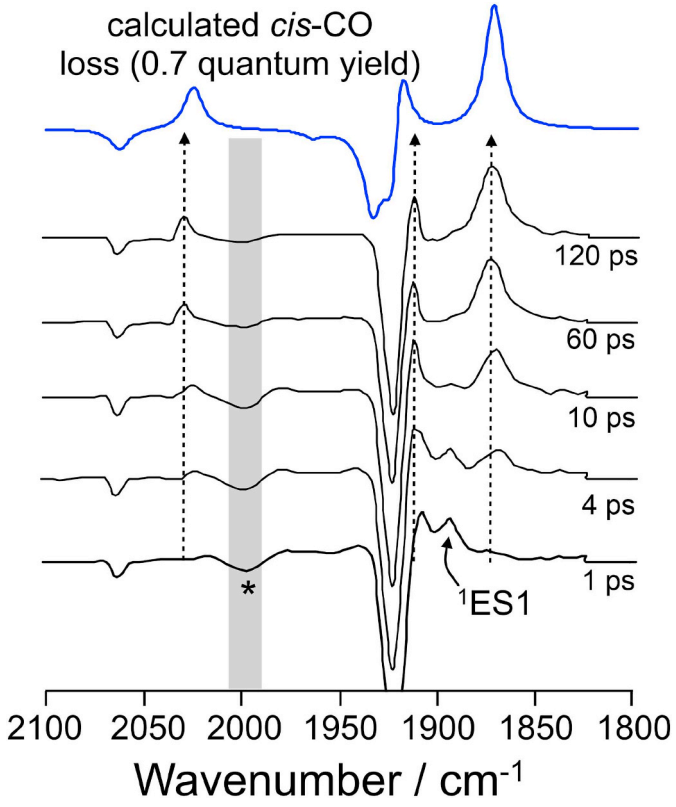

Fig. 4. Picosecond time-resolved infrared spectra obtained at 1, 4, 10, 60, and 120 ps following excitation of $[(CO)_5WC(NC_4H_8)Me]$ in *n*-heptane solution (black spectra) and the calculated difference spectrum obtained by subtracting the simulated spectrum of $[(CO)_5WC(NC_4H_8)Me]$ from *cis*-$[(CO)_4WC(NC_4H_8)Me]$ in *n*-heptane assuming a quantum yield of 0.7 (blue spectrum), the vertical dashed arrows shows the formation of product bands and the shaded area (*) indicates a region of apparent depletion which is an artefact of a detector fault.

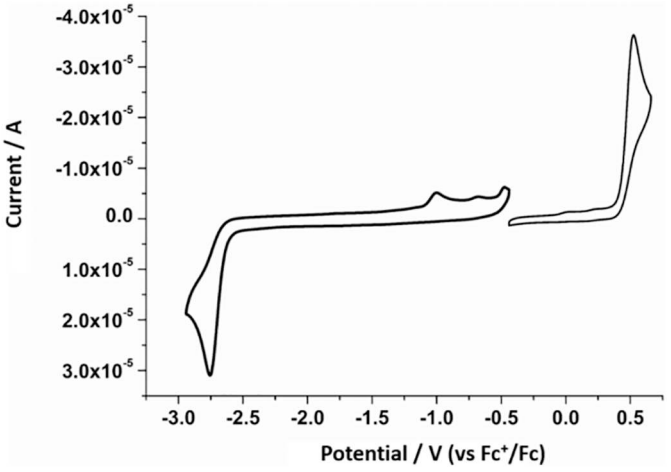

Fig. 5. Cyclic voltammogram depicting the oxidation and reduction of $[(CO)_5WC(NC_4H_8)Me]$ in dry CH_3CN and 0.1 M nBu_4PF_6, Scan rate = 0.1 V/ s.

The three anodic processes are observed in the range of −1.0 to −0.4 V are followed with the reduction of the complex (shown in Fig. 5). In the present study, electrochemical initiation of CO release from a 1 mM solution of the complex in CH_3CN was confirmed and is shown in Fig. 6(b), over five intervals approximately 20 min apart over 1.5 h of controlled potential electrolysis (E = +0.87, vs. Fc/Fc$^+$). In these electrolysis experiments, CO loss over the course of the experiment is ~1 molecule of CO per molecule of complex, which is similar to

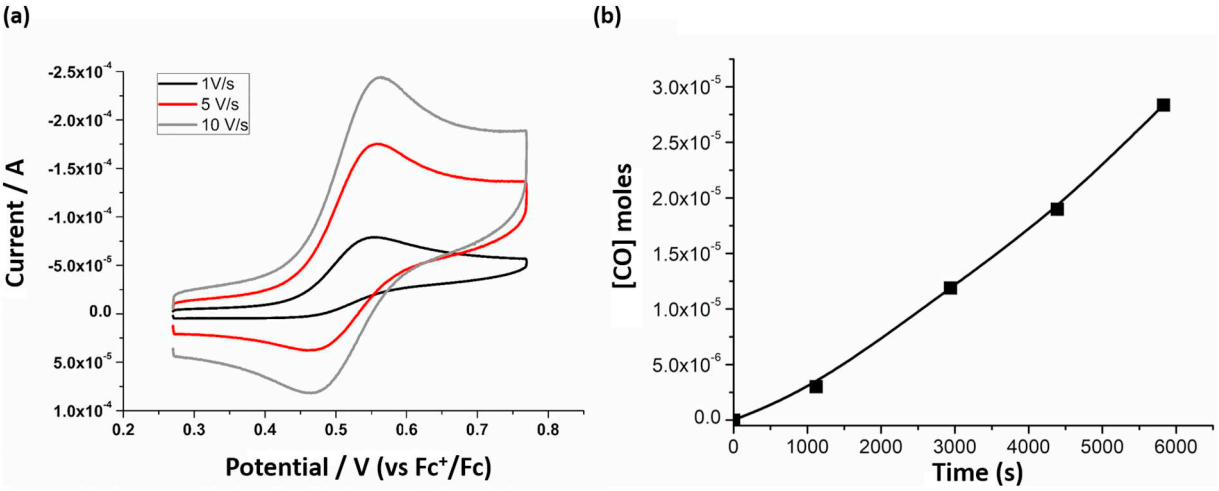

Fig. 6. (a). Scan rate dependence of the first oxidation process for $(CO)_5WC(NC_4H_8)Me$ in 0.1 M $TBAPF_6$ in CH_3CN, vs. Fc/Fc^+. CVs for scan rate of 1.0, 5.0 and 10.0 V/s shown here. (b). Time-dependent electrochemically induced CO release from $[(CO)_5WC(NC_4H_8)Me]$ (1 mM) in CH_3CN.

other studies performed by us on chromium analogues [18,55].

3.3. Bactericidal activity of $[(CO)_5WC(NC_4H_8)Me]$

The TRIR studies indicated that the quantum yield of photoinduced CO-loss from $[(CO)_5WC(NC_4H_8)Me]$ is high at ~70%, and therefore suggests this complex is an ideal candidate to be used as a CO releasing compound with antibacterial properties.

$[(CO)_5WC(NC_4H_8)CH_3]$ demonstrated concentration dependent bactericidal, against *S. aureus*, when photo-activated for 1 h at 355 nm (Fig. 7). The greatest differential between photo-activation and no irradiation was observed at 200 μM. Apparent low-level killing activity (10–20%) was observed in the absence of light, over the concentration range investigated. To investigate the dependence of photoactivated bactericidal activity on CO-release, bovine haemoglobin (Hb), a high affinity CO scavenger was added to the assays [43]. The bactericidal activity decreased by ~65%, following the addition of Hb, thereby indicating the cytotoxic role of CO (Fig. S3). Singlet oxygen measurements (see ESI) indicated no evidence for the formation of $^1O_2$, which may also photodynamically inactivate bacteria (Fig. S2). For this complex, the cytotoxicity was attributed predominantly to CO release and to a lesser extent, tungsten carbonyl degradation products.

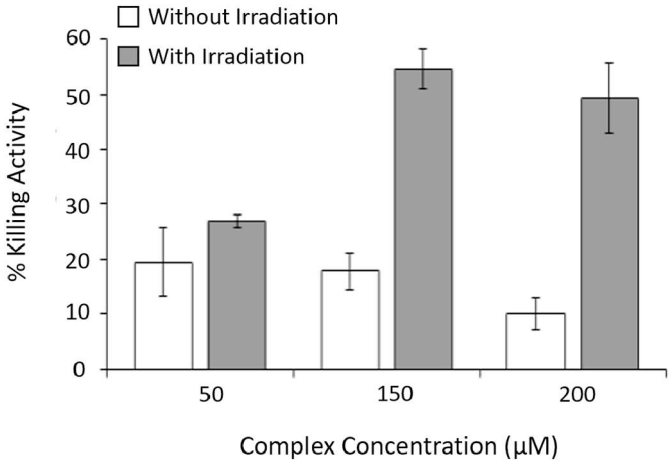

Fig. 7. Photo-activated bactericidal activity of $[(CO)_5WC(NC_4H_8)CH_3]$ against *S. aureus* ATCC25923 in PBS, pH 7.4. Activity in the absence of irradiation (light grey bars) and with irradiation for 1 h, λ = 355 nm (dark grey bars) over the concentration of catalyst ranging from 50 μM to 200 μM. Assays were performed in duplicate on 3 separate occasions and percentage killing activity was calculated from CFU/ml in the presence of complex relative to CFU/ml from control assays (assay with no complex). The mean value and standard error are shown. In the absence of complex, no killing effect was observed following irradiation (CFU/ml = 141,550 ± 50,113 - no light Vs 196,700 ± 54,591-with light).

4. Conclusion

The tungsten based amino carbene complex, $[(CO)_5WC(NC_4H_8)Me]$ was assessed for both photo, and electrochemical CO-release. The CO-loss photoproduct *cis*-$[(CO)_4WC(NC_4H_8)Me]$ was generated via the formation of an excited state over 80 ps, as evident by picosecond time resolved infrared spectroscopy, and was further supported by quantum chemical calculations. From cyclic voltammetry studies, the complex also releases CO, but this approach is less efficient than when a photo-stimuli is used. The potential of this complex for antibacterial activity was assessed using a representative Gram-positive bacteria, *S. aureus*. Enhanced antibacterial activity was evident following irradiation, thereby indicating the potential of such complexes to act as antibacterial agents. CO trapping studies indicate that CO is predominantly responsible for the bactericidal activity. While carbon monoxide-releasing molecules have been shown to act as promising antimicrobials against several pathogens over the last decade [39,73,74], the mode of action is not fully clear and depending on the compound, multiple interactions with intracellular targets may occur that result in cell membrane perturbations, inhibition of DNA repair or iron chelation. Determining the fate of CO and its mechanisms of interaction with bacteria was beyond the scope of this work. However, for other CORMs Nobre et al. [43] showed that CO gas does not dissolve in the medium following its release, inferring that CO interacts directly with intracellular targets once released. Furthermore, for one CO-RM, tetraethylammonium molybdenum pentacarbonyl bromide (ALF 062) they noted accumulation of Mo inside *E. coli* cells suggesting that this CORM transports CO across the membranes for intracellular delivery.

One of the key challenges in using CO as a therapeutic is to control its delivery, such as using light or a redox stimulus, the approaches taken in this study. In our preliminary antimicrobial studies, a high quantum yield for photo-induced CO release, resulted in modest antibacterial activity against *S. aureus*. However, the potential of this approach for clinical applications requiring controlled delivery of antimicrobial activity was demonstrated.

Declaration of competing interest

There is no conflict of interest concerning the results stated in this manuscript.

The funding sources have been stated in the manuscript.

Acknowledgements

The authors thank the Amsterdam Laboratory under EU access-LLAMS-1961. We would also like to thank the Irish Research Council RS/2012/341 (SM), a SFI-13/TIDA/E2763 grant (YH and MTP), and the Health Research Board-Diabetes Ireland Research Alliance HRBMRCG-2018-01 (AR) for financial support. We would also like to thank the DJEI/DES/SFI/HEA Irish Centre for High-End Computing (ICHEC) for the provision of computational facilities and support.

Appendix A. Supplementary data

Supplementary data to this article can be found online at https://doi.org/10.1016/j.jinorgbio.2020.111071.

References

[1] H. Váňová, T. Tobrman, M. Babor, D. Dvořák, Reaction of lithiated thiophene-derived aminocarbene complexes with inorganic halides: preparation of a heteroatom containing mono- and multicarbene complexes, J. Organomet. Chem. 882 (2019) 90–95, https://doi.org/10.1016/j.jorganchem.2018.12.015.

[2] K.H. Dötz, J. Stendel, Fischer carbene complexes in organic synthesis: metal-assisted and metal-templated reactions, Chem. Rev. 109 (2009) 3227–3274, https://doi.org/10.1021/cr900034e.

[3] F. Hu, J. Yang, Y. Xia, C. Ma, H. Xia, Y. Zhang, J. Wang, C-H bond functionalization of benzoxazoles with chromium(0) Fischer carbene complexes, Organometallics. 35 (2016) 1409–1414, https://doi.org/10.1021/acs.organomet.6b00008.

[4] K. Endo, Development of neighboring electrophilic activation of active center in catalytic reactions via organometallic intermediates, Bull. Chem. Soc. Jpn. 90 (2017) 649–661, https://doi.org/10.1246/bcsj.20170015.

[5] Y.G.N. Iwasawa, K. Kyokaishi, Fischer-type carbene complexes in organic synthesis, J. Synth. Org. Chem. 56 (1998) 413–423, https://doi.org/10.5059/yukigoseikyokaishi.56.413.

[6] J. Santamaría, E. Aguilar, Beyond Fischer and Schrock carbenes: non-heteroatom-stabilized group 6 metal carbene complexes-a general overview, Org. Chem. Front. 3 (2016) 1561–1588, https://doi.org/10.1039/c6qo00206d.

[7] I. Fernández, F.P. Cossío, M.A. Sierra, Photochemistry of group 6 Fischer carbene complexes: beyond the photocarbonylation reaction, Acc. Chem. Res. 44 (2011) 479–490, https://doi.org/10.1021/ar100159h.

[8] I. Fernández, M.A. Sierra, M. Gómez-Gallego, M.J. Mancheño, F.P. Cossío, The photochemical reactivity of the “photo-inert” tungsten (Fischer) carbene complexes, Angew. Chemie-Int. Ed. 45 (2005) 125–128, https://doi.org/10.1002/anie.200501590.

[9] I. Fernández, M.A. Sierra, M.J. Mancheño, M. Gómez-Gallego, F.P. Cossío, The noncarbonylative photochemistry of group 6 Fischer carbene complexes, Eur. J. Inorg. Chem. (2008) 2454–2462, https://doi.org/10.1002/ejic.200800146.

[10] Z.F. Zhang, M. Der Su, Mechanistic study for the photochemical reactions of d^6 M $(CO)_5(CS)$ (M = Cr, Mo, and W) complexes, ACS Omega 2 (2017) 2813–2826, https://doi.org/10.1021/acsomega.7b00380.

[11] L.S. Hegedus, Transition metals in the synthesis and functionalization of indoles, Angew. Chemie Int. Ed. English. 27 (1988) 1113–1226, https://doi.org/10.1002/anie.197506551.

[12] L.S. Hegedus, Synthesis of amino acids and peptides using chromium carbene complex photochemistry, Acc. Chem. Res. 28 (1995) 299–305, https://doi.org/10.1021/ar00055a003.

[13] S. McMahon, S. Amirjalayer, W.J. Buma, Y. Halpin, C. Long, A.D. Rooney, S. Woutersen, M.T. Pryce, An investigation into the photochemistry of, and the electrochemically induced CO-loss from, $[(CO)_5MC(OMe)Me]$(M = Cr or W) using lowerature matrix isolation, picosecond infrared spectroscopy, cyclic voltammetry, and time-dependent density functional theory, Dalton Trans. 44 (2015) 15424–15434, https://doi.org/10.1039/c5dt01568e.

[14] S.C. Nguyen, J.P. Lomont, M.C. Zoerb, P.V. Pham, J.F. Cahoon, C.B. Harris, Direct observation of metal ketenes formed by photoexcitation of a Fischer carbene using ultrafast infrared spectroscopy, Organometallics 33 (2014) 6149–6153, https://doi.org/10.1021/om500795b.

[15] M.L. Gallagher, J.B. Greene, A.D. Rooney, Matrix isolation study into the mechanism of photoinduced cyclization reactions of chromium carbenes, Organometallics 16 (1997) 5260–5268.

[16] A. Hafner, L.S. Hegedus, G. deWeck, B. Hawkins, K.H. Dötz, Chromium-53 nuclear magnetic resonance studies of pentacarbonylchromium-carbene complexes, J. Am. Chem. Soc. 110 (1988) 8413–8421, https://doi.org/10.1021/ja00233a018.

[17] K.O. Doyle, M.L. Gallagher, M.T. Pryce, A.D. Rooney, A matrix isolation and flash photolysis study of the cyclization reactions of chromium amino carbenes, J. Organomet. Chem. 617 (2001) 269–279, https://doi.org/10.1192/bjp.111.479.1009-a.

[18] S. McMahon, J. Rochford, Y. Halpin, J.C. Manton, E.C. Harvey, G.M. Greetham, I.P. Clark, A.D. Rooney, C. Long, M.T. Pryce, Controlled CO release using photochemical, thermal and electrochemical approaches from the amino carbene complex $[(CO)_5CrC(NC_4H_8)CH_3]$, Phys. Chem. Chem. Phys. 16 (2014) 21230–21233, https://doi.org/10.1039/c4cp03758h.

[19] A.D. Rooney, J.J. McGarvey, K.C. Gordon, R.A. McNicholl, U. Schubert, W. Hepp, Laser photochemistry and transient Raman spectroscopy of silyl-substituted Fischer-type carbene complexes, Organometallics 12 (1993) 1277–1282, https://doi.org/10.1021/om00028a050.

[20] H. Yan, J. Du, S. Zhu, G. Nie, H. Zhang, Z. Gu, Y. Zhao, Emerging delivery strategies of carbon monoxide for therapeutic applications: from CO gas to CO releasing nanomaterials, Small 15 (2019) 1904382–1904387, https://doi.org/10.1002/smll.201904382 (doi:10.1002/smll.201904382).

[21] D.G. Levitt, M.D. Levitt, Carbon monoxide: a critical quantitative analysis and review of the extent and limitations of its second messenger function, Clin. Pharmacol. Adv. Appl. 7 (2015) 37–56, https://doi.org/10.2147/CPAA.S79626.

[22] H.H. Kim, S. Choi, Therapeutic aspects of carbon monoxide in cardiovascular disease, Int. J. Mol. Sci. 19 (2018) 2381–2393, https://doi.org/10.3390/ijms19082381.

[23] L. Flanagan, R.R. Steen, K. Saxby, M. Klatter, B.J. Aucott, C. Winstanley, I.J.S. Fairlamb, J.M. Lynam, A. Parkin, V.P. Friman, The antimicrobial activity of a carbon monoxide releasing molecule (EBOR-CORM-1) is shaped by intraspecific variation within Pseudomonas aeruginosa populations, Front. Microbiol. 9 (2018) 1–11, https://doi.org/10.3389/fmicb.2018.00195.

[24] M. Faizan, N. Muhammad, K.U.K. Niazi, Y. Hu, Y. Wang, Y. Wu, H. Sun, R. Liu, W. Dong, W. Zhang, Z. Gao, CO-releasing materials: an emphasis on therapeutic implications, as release and subsequent cytotoxicity are the part of therapy, Materials (Basel) 12 (2019) 1643–1684, https://doi.org/10.3390/ma12101643.

[25] A.E. Pierri, P.J. Huang, J.V. Garcia, J.G. Stanfill, M. Chui, G. Wu, N. Zheng, P.C. Ford, A photoCORM nanocarrier for CO release using NIR light, Chem. Commun. 51 (2015) 2072–2075, https://doi.org/10.1039/c4cc06766e.

[26] Z. Li, A.E. Pierri, P.J. Huang, G. Wu, A.V. Iretskii, P.C. Ford, Dinuclear PhotoCORMs: dioxygen-assisted carbon monoxide uncaging from long-wavelength-absorbing metal-metal-bonded carbonyl complexes, Inorg. Chem. 56 (2017) 6094–6104, https://doi.org/10.1021/acs.inorgchem.6b03138.

[27] M.A. Wright, J.A. Wright, PhotoCORMs: CO release moves into the visible, Dalton Trans. 45 (2016) 6801–6811, https://doi.org/10.1039/c5dt04849d.

[28] C. Motterlini, R. Clark, J. Foresti, R. Sarathchandra, P. Mann, B. Green, Carbon monoxide-releasing molecules - characterization of biochemical and vascular activities, Circ. Res. 90 (2002) E17–E24.

[29] R. Dale Rimmer, H. Richter, P.C. Ford, A photochemical precursor for carbon monoxide release in aerated aqueous media, Inorg. Chem. 49 (2010) 1180–1185, https://doi.org/10.1021/ic902147n.

[30] P. Rudolf, F. Kanal, J. Knorr, C. Nagel, J. Niesel, T. Brixner, U. Schatzschneider, P. Nuernberger, Ultrafast photochemistry of a manganese-tricarbonyl CO-releasing molecule (CORM) in aqueous solution, J. Phys. Chem. Lett. 4 (2013) 596–602, https://doi.org/10.1021/jz302061q.

[31] S. Hubick, A. Jayaraman, A. McKeen, S. Reid, J. Alcorn, J. Stavrinides, B.T. Sterenberg, A potent synthetic inorganic antibiotic with activity against drug-resistant pathogens, Sci. Rep. 7 (2017) 1–7, https://doi.org/10.1038/srep41999.

[32] H.M. Southam, T.W. Smith, R.L. Lyon, C. Liao, C.R. Trevitt, L.A. Middlemiss, F.L. Cox, J.A. Chapman, S.F. El-Khamisy, M. Hippler, M.P. Williamson, P.J.F. Henderson, R.K. Poole, A thiol-reactive Ru(II) ion, not CO release, underlies the potent antimicrobial and cytotoxic properties of CO-releasing molecule-3, Redox Biol. (2018) 114–123, https://doi.org/10.1016/j.redox.2018.06.008.

[33] X. Wang, K. Maeda, A. Thomas, K. Takanabe, G. Xin, J.M. Carlsson, K. Domen, M. Antonietti, A Metal-free Polymeric Photocatalyst for Hydrogen Production From Water Under Visible Light, 8 (2009), pp. 6–10, https://doi.org/10.1038/NMAT2317.

[34] W.Q. Zhang, A.C. Whitwood, I.J.S. Fairlamb, J.M. Lynam, Group 6 carbon monoxide-releasing metal complexes with biologically- compatible leaving groups, Inorg. Chem. 49 (2010) 8941–8952, https://doi.org/10.1021/ic101230j.

[35] J. Marhenke, A.E. Pierri, M. Lomotan, P.L. Damon, P.C. Ford, C. Works, Flash and continuous photolysis kinetic studies of the iron–iron hydrogenase model (μ-pdt)$[Fe(CO)_3]_2$ in different solvents, Inorg. Chem. 50 (2011) 11850–11852, https://doi.org/10.1021/ic201523r.

[36] W.-Q. Zhang, A.J. Atkin, I.J.S. Fairlamb, A.C. Whitwood, J.M. Lynam, Synthesis and reactivity of molybdenum complexes containing functionalized alkynyl ligands: a photochemically activated CO-releasing molecule (PhotoCO-RM), Organometallics 30 (2011) 4643–4654, https://doi.org/10.1021/om200495h.

[37] R. Motterlini, J.E. Clark, R. Foresti, P. Sarathchandra, B.E. Mann, C.J. Green, Carbon monoxide-releasing molecules: characterization of biochemical and vascular activities, Circ. Res. 90 (2002) e17–e24, https://doi.org/10.1161/hh0202.104530.

[38] L.S. Nobre, H. Jeremias, C.C. Romão, L.M. Saraiva, Examining the antimicrobial activity and toxicity to animal cells of different types of CO-releasing molecules, Dalton Trans. 45 (2016) 1455–1466, https://doi.org/10.1039/C5DT02238J.

[39] J.S. Ward, R. Morgan, J.M. Lynam, I.J.S. Fairlamb, J.W.B. Moir, Toxicity of tryptophan manganese(I) carbonyl (Trypto-CORM), against Neisseria gonorrhoeae, Med. Chem. Commun. 8 (2017) 346–352, https://doi.org/10.1039/C6MD00603E.

[40] A.M. Mansour, Green-light-induced PhotoCORM: lysozyme binding affinity towards MnI and ReI carbonyl complexes and biological activity evaluation, Eur. J. Inorg. Chem. 2018 (2018) 4805–4811, https://doi.org/10.1002/ejic.201801055.

[41] A.M. Mansour, RuII–carbonyl photoCORMs with N,N-benzimidazole bidentate ligands: spectroscopic, lysozyme binding affinity, and biological activity evaluation, Eur. J. Inorg. Chem. 2018 (2018) 852–860, https://doi.org/10.1002/ejic.201701341.

[42] M.A. Gonzales, P.K. Mascharak, Photoactive metal carbonyl complexes as potential agents for targeted CO delivery, J. Inorg. Biochem. 133 (2014) 127–135, https://doi.org/10.1016/J.JINORGBIO.2013.10.015.

[43] L.S. Nobre, J.D. Seixas, C.C. Romão, L.M. Saraiva, Antimicrobial action of carbon monoxide-releasing compounds, Antimicrob. Agents Chemother. 51 (2007) 4303–4307, https://doi.org/10.1128/AAC.00802-07.

[44] L. Flanagan, R.R. Steen, K. Saxby, M. Klatter, B.J. Aucott, C. Winstanley, I.J.S. Fairlamb, J.M. Lynam, A. Parkin, V.-P. Friman, The antimicrobial activity of a carbon monoxide releasing molecule (EBOR-CORM-1) is shaped by intraspecific variation within Pseudomonas aeruginosa populations, Front. Microbiol. 9 (2018) 195 https://www.frontiersin.org/article/10.3389/fmicb.2018.00195.

[45] P. Güntzel, C. Nagel, J. Weigelt, J.W. Betts, C.A. Pattrick, H.M. Southam, R.M. La Ragione, R.K. Poole, U. Schatzschneider, Biological activity of manganese(i) tricarbonyl complexes on multidrug-resistant gram-negative bacteria: from functional studies to in vivo activity in Galleria mellonella, Metallomics 11 (2019) 2033–2042, https://doi.org/10.1039/C9MT00224C.

[46] C. Sahlberg Bang, R. Kruse, K. Johansson, K. Persson, Carbon monoxide releasing molecule-2 (CORM-2) inhibits growth of multidrug-resistant uropathogenic Escherichia coli in biofilm and following host cell colonization, BMC Microbiol. 16 (2016) 1–10, https://doi.org/10.1186/s12866-016-0678-7.

[47] K.S. Egorova, V.P. Ananikov, Toxicity of metal compounds: knowledge and myths, Organometallics 36 (2017) 4071–4090, https://doi.org/10.1021/acs.organomet.7b00605.

[50] J.A. Lemire, J.J. Harrison, R.J. Turner, Antimicrobial activity of metals: mechanisms, molecular targets and applications, Nat. Rev. Microbiol. 11 (2013) 371–384, https://doi.org/10.1038/nrmicro3028.

[51] M. Desmard, K.S. Davidge, O. Bouvet, D. Morin, D. Roux, R. Foresti, J.D. Ricard, E. Denamur, R.K. Poole, P. Montravers, R. Motterlini, J. Boczkowski, A carbon monoxide-releasing molecule (CORM-3) exerts bactericidal activity against Pseudomonas aeruginosa and improves survival in an animal model of bacteraemia, FASEB J. 23 (2009) 1023–1031, https://doi.org/10.1096/fj.08-122804.

[52] L.K. Wareham, S. McLean, R. Begg, N. Rana, S. Ali, J.J. Kendall, G. Sanguinetti, B.E. Mann, R.K. Poole, The broad-spectrum antimicrobial potential of [Mn$(CO)_4(S_2CNMe(CH_2CO_2H))$], a water-soluble CO-releasing molecule (CORM-401): intracellular accumulation, transcriptomic and statistical analyses, and membrane polarization, Antioxid. Redox Signal. 28 (2017) 1286–1308, https://doi.org/10.1089/ars.2017.7239.

[53] N. Rana, H.E. Jesse, M. Tinajero-Trejo, J.A. Butler, J.D. Tarlit, M.L. von und zur Muhlen, C. Nagel, U. Schatzschneider, R.K. Poole, A manganese photosensitive tricarbonyl molecule [$Mn(CO)_3$(tpa-κ_3 N)]Br enhances antibiotic efficacy in a multidrug-resistant Escherichia coli, Microbiology 163 (2017) 1477–1489, https://doi.org/10.1099/mic.0.000526.

[54] L.K. Wareham, R.K. Poole, M. Tinajero-Trejo, CO-releasing metal carbonyl compounds as antimicrobial agents in the post-antibiotic era, J. Biol. Chem. 290 (2015) 18999–19007, https://doi.org/10.1074/jbc.R115.642926.

[55] D.J. Frisch, M.J. Trucks, G.W. Schlegel, H.B. Scuseria, G.E. Robb, M.A. Cheeseman, J.R. Scalmani, G. Barone, V. Petersson, G.A. Nakatsuji, H. Li, X. Caricato, M. Marenich, A.V. Bloino, J. Janesko, B.G. Gomperts, R. Mennucci, B. Hratch, Gaussian 16, Revision B.01, Gaussian 16, Revis. B.01, 2.0 Gaussian, Inc, Wallingford CT, 2016.

[56] A.D. Becke, Density-functional exchange-energy approximation with correct asymptotic behavior, Phys.Rev.A. 38 (1988) 3098–3100, https://doi.org/10.1103/PhysRevA.38.3098.

[57] R.G.P.C. Lee, W. Yang, Development of the Colle-Salvetti correlation-energy formula into a functional of the electron density, Phys.Rev B. 37 (1988) 785–789, https://doi.org/10.1103/PhysRevB.37.785.

[58] H.P.B. Miehlich, A. Savin, H. Stoll, Results obtained with the correlation-energy density functionals of Becke and Lee, Yang and Parr, Chem. Phys. Lett. 157 (1989) 200–206, https://doi.org/10.1016/0009-2614(89)87234-3.

[59] F. Weigend, Accurate Coulomb-fitting basis sets for H to Rn, Phys. Chem. Chem. Phys. 8 (2006) 1057–1065, https://doi.org/10.1039/b515623h.

[60] F. Weigend, R. Ahlrichs, Balanced basis sets of split valence, triple zeta valence and quadruple zeta valence quality for H to Rn: design and assessment of accuracy, Phys. Chem. Chem. Phys. 7 (2005) 3297–3305, https://doi.org/10.1039/b508541a.

[61] J. Tomasi, B. Mennucci, R. Cammi, Quantum mechanical continuum solvation models, Chem. Rev. 105 (2005) 2999–3093, https://doi.org/10.1021/cr9904009.

[62] R. Bauernschmitt, R. Ahlrichs, Treatment of electronic excitations within the adiabatic approximation of time dependent density functional theory, Chem. Phys. Lett. 256 (1996) 454–464, https://doi.org/10.1016/0009-2614(96)00440-X.

[63] R.E. Stratmann, G.E. Scuseria, M.J. Frisch, An efficient implementation of time-dependent density-functional theory for the calculation of excitation energies of large molecules, J. Chem. Phys. 109 (1998) 8218–8224, https://doi.org/10.1063/1.477483.

[64] E. Connor, J. Fischer, Transition-metal carbene complexes. Part XII. Substituent and steric effects in aminocarbene complexes of chromium, J. Chem. Soc. A 4 (1969) 578–584.

[65] C. Cedillo-Cruz, A. Carmen Ortega-Alfaro, M. Lopez-Cortes, J.G. Alfredo Toscano, R. Guillermo Penieres-Carrillo, J. Alvarez-Toledano, Synthesis of Fischer type-carbene complexes containing a coordinated thioimidate structural motif, Dalton Trans. 41 (2012) 10568–10575.

[66] A. Doyle, K. Gallagher, M. Pryce, M. Rooney, A matrix isolation and flash photolysis study of the cyclization reactions of chromium amino carbenes, J. Organomet. Chem. 617 (2001) 269–279.

[67] M.A.H. Alamiry, N.M. Boyle, C.M. Brookes, M.W. George, L. Conor, P. Portius, M.T. Pryce, K.L. Ronayne, X.Z. Sun, M. Towrie, Q.V. Khuong, Unusually slow photodissociation of CO from (η^6-C_6H_6)Cr$(CO)_3$ (M = Cr or Mo): a time-resolved infrared, matrix isolation, and DFT investigation, Organometallics 28 (2009) 1461–1468, https://doi.org/10.1021/om800925s.

[68] N. Ben Amor, S. Villaume, D. Maynau, C. Daniel, The electronic spectroscopy of transition metal carbonyls: the tough case of Cr(CO)6, Chem. Phys. Lett. 421 (2006) 378–382, https://doi.org/10.1016/j.cplett.2006.02.002.

[69] C. Pollak, A. Rosa, E.J. Baerends, Cr-CO photodissociation in Cr(CO)6: reassessment of the role of ligand-field excited states in the photochemical dissociation of metal-ligand bonds, J. Am. Chem. Soc. 119 (1997) 7324–7329, https://doi.org/10.1021/ja970592u.

[70] I. Hoskovcová, J. Roháčová, L. Meca, T. Tobrman, D. Dvořák, J. Ludvík, Electrochemistry of chromium(0)–aminocarbene complexes: the use of intramolecular interaction LFER for characterization of the oxidation and reduction centre of the complex, Electrochim. Acta 50 (2005) 4911–4915, https://doi.org/10.1016/J.ELECTACTA.2004.12.047.

[71] M. Landman, R. Liu, R. Fraser, P.H. van Rooyen, J. Conradie, Fac and mer dppe-substituted Fischer carbene complexes of chromium: X-ray, DFT and electrochemical study, J. Organomet. Chem. 752 (2014) 171–182, https://doi.org/10.1016/J.JORGANCHEM.2013.12.003.

[72] P.V. Simpson, C. Nagel, H. Bruhn, U. Schatzschneider, Antibacterial and antiparasitic activity of manganese(I) tricarbonyl complexes with ketoconazole, miconazole, and clotrimazole ligands, Organometallics 34 (2015) 3809–3815, https://doi.org/10.1021/acs.organomet.5b00458.

[73] K.S. Davidge, G. Sanguinetti, C.H. Yee, A.G. Cox, C.W. McLeod, C.E. Monk, B.E. Mann, R. Motterlini, R.K. Poole, Carbon monoxide-releasing antibacterial molecules target respiration and global transcriptional regulators, J. Biol. Chem. 284 (2009) 4516–4524, https://doi.org/10.1074/jbc.M808210200.

[74] S.M. Carvalho, J. Marques, C.C. Romão, L.M. Saraiva, Metabolomics of Escherichia coli treated with the antimicrobial carbon monoxide-releasing molecule CORM-3 reveals tricarboxylic acid cycle as major target, Antimicrob. Agents Chemother. 63 (2019), https://doi.org/10.1128/AAC.00643-19 e00643-19.